Comparison of the perturbative convergence with multireference Möller–Plesset, Epstein–Nesbet, forced degenerate and optimized zeroth order partitionings: The excited BeH2 surface

Rajat K. Chaudhuri, James P. Finley, and Karl F. Freed

Articles you may be interested in

A spin-adapted size-extensive state-specific multi-reference perturbation theory with various partitioning schemes. II. Molecular applications
J. Chem. Phys. **136**, 024106 (2012); 10.1063/1.3672085

Quadratically convergent algorithm for orbital optimization in the orbital-optimized coupled-cluster doubles method and in orbital-optimized second-order Møller-Plesset perturbation theory
J. Chem. Phys. **135**, 104103 (2011); 10.1063/1.3631129

Comparative study of multireference perturbative theories for ground and excited states
J. Chem. Phys. **131**, 204104 (2009); 10.1063/1.3265769

Comparison of low-order multireference many-body perturbation theories
J. Chem. Phys. **122**, 134105 (2005); 10.1063/1.1863912

Multireference perturbation theory with optimized partitioning. I. Theoretical and computational aspects
J. Chem. Phys. **118**, 8197 (2003); 10.1063/1.1563618

Comparison of the perturbative convergence with multireference Möller–Plesset, Epstein–Nesbet, forced degenerate and optimized zeroth order partitionings: The excited BeH$_2$ surface

Rajat K. Chaudhuri, James P. Finley, and Karl F. Freed

The James Franck Institute and the Department of Chemistry, The University of Chicago, Chicago, Illinois 60637

High order perturbation energies are computed for excited $^1A_1$ states of BeH$_2$ at geometries near the Be→H$_2$ symmetric insertion transition state. The equations of multireference perturbation theory are solved through 30th order to study the difficulties in selecting the appropriate zeroth order Hamiltonian, orbitals, orbital energies, and reference functions for the computations of smooth molecular potential energy surfaces. The origin of the perturbative divergence produced by Möller–Plesset and Epstein–Nesbet partitionings is analyzed using a conceptually simple two-state model constructed using one state each from the reference and orthogonal spaces. The optimized zeroth order partitioning scheme (OPT) for double reference space computations with configurations $1a_1^2 2a_1^2 3a_1^2$ and $1a_1^2 2a_1^2 1b_2^2$ produces a truly convergent perturbation expansion through 30th order. The OPT energies are accurate in low orders as compared to the exact (197 dimensional) solution within the basis. The forced valence orbital degeneracy partitioning method (FD) also generates a truly convergent expansion for the same double reference space calculation, with slightly poorer low order energies than the OPT scheme. The BeH$_2$ system facilitates the consideration of larger reference spaces (constructed using three through six orbitals) where the FD method produces highly accurate energies in low orders despite the asymptotic nature of the FD perturbation expansion. The ''delayed'' perturbative divergence behavior with the FD partitioning scheme (for large reference spaces) is shown to occur due to the incorrect ordering between the zeroth order energies of some reference and complementary space levels. © *1997 American Institute of Physics.* [S0021-9606(97)01808-4]

I. INTRODUCTION

Accurate theories for the calculation of atomic and molecular electronic structure can be classified broadly into variational and nonvariational varieties. The nonvariational approaches include the single reference configuration (SR) many-body perturbation theory (MBPT),[1–4] which is a widely used and convenient procedure for a significant range of problems. The nonvariational method can be classified further into (a) perturbative and (b) nonperturbative categories that invoke different philosophies and possess different advantages. The perturbative approach relies on an order-by-order expansion which retains all excitation processes required at each order, whereas the nonvariational, nonperturbative approach (e.g., the coupled cluster method[5–7]) treats particular types of excitations to all orders. Both of these categories of nonvariational methods have the important virtue of maintaining size extensivity.

Despite its great success in treating electron correlation for many types of systems, the SR-MBPT method is often inefficient (poorly convergent or even divergent) for quaside-generate situations or for highly open shell systems where more than one reference configuration is important. Thus problems frequently arise in calculating excited state energies and potential energy surfaces near transition states or bond breaking regions. The use of an unrestricted Hartree–Fock reference function overcomes a portion of the convergence problem, especially near the bond breaking regions.

However, the perturbed wave function is spin contaminated, and the overall accuracy becomes degraded,[8–10] especially when the single reference function is an excited state.

Several different multireference configuration MBPT (MR-MBPT) approaches (maintaining the correct spin symmetry)[11–19] have been proposed as a natural remedy to the deficiencies of the SR-MBPT method. The fundamental idea is to construct an effective Hamiltonian whose eigenvalues coincide with a subset of the eigenvalues of the exact Hamiltonian. The first size-extensive MR-MBPT formulation of Brandow[11] employs a complete reference space (often called a complete active space). The choice of a complete active space facilitates the proof of the linked cluster theorem which guarantees that the effective Hamiltonian H_{eff} has a connected diagrammatic expansion and consequently that the eigenvalues of H_{eff}, the energies, are size extensive.

While the MR-MBPT formalism resolves several shortcomings of the SR-MBPT method, it introduces another problem that has been called the ''intruder state problem.'' Schucan and Weidenmüller hypothesize that multireference perturbation expansions must diverge whenever an exact state, which is predominantly composed of configurations outside the reference space, appears within the energy spectrum of the exact states that are predominantly represented by reference space states.[20,21] This conjecture emerges from using a zeroth order Hamiltonian in which the zeroth order energies of the reference and orthogonal space states are not

permitted to overlap. We have demonstrated that this pessimistic conclusion is *not* valid if the restriction is lifted to allow an energy overlap between the zeroth order reference and orthogonal spaces. For example, the optimized partitioning method (OPT) computations for the beryllium atom[22] place the reference space $|1s^2 2s^2\rangle$ configuration state function (CSF) above the orthogonal space $|1s^2 2s 3s\rangle$ (Rydberg) CSF. Besides converging to the ground state energy, the perturbative computation with two reference states converges to the *second* excited state and not the first.

An alternative solution for avoiding this problem is to use MR-MBPT with an incomplete model space, as first developed and applied by Hose and Kaldor.[23] Unlike the complete active space theories, there have been lengthy disputes[24,25] regarding the size extensivity of the incomplete model space theories. Mukherjee[26,27] provides a formal resolution of the size-extensivity problem for the incomplete model space theories by describing a ''proper size-extensive normalization.''

For all practical purposes, actual perturbative computations require the truncation of the perturbative expansion, and this truncation is only meaningful if the perturbation series either converges rapidly or, at least, converges rapidly in an asymptotic sense. The MR-MBPT method frequently suffers from a poor convergence problem unless an appropriate reference space is selected. This proper choice of reference space becomes important in computing smooth accurate potential energy surfaces as evidenced by the general belief that the use of a single common active space is essential for calculating the potential energy surface over an interesting range of geometries. It is likewise widely believed that the MR-MBPT method is incapable of providing a rapidly convergent perturbation series for the entire range of geometries. The latter belief follows from the expectation that some reference space states may escape intruder state problems for certain ranges of geometries but become plagued by these problems for other geometries. Similar questions have been raised for the intermediate Hamiltonian method, a variant of MR-MBPT.[28]

It is well known that perturbative convergence depends strongly on the choice of the zeroth order Hamiltonian H_0, i.e., on the partitioning of the exact Hamiltonian between H_0 and the perturbation V.[29–31] The two general categories of partitioning are called generalized Möller–Plesset (MP) and generalized Epstein–Nesbet (EN) partitionings. The generalized MP partitioning utilizes a ''sum over orbitals'' treatment, whereas the generalized EN partitioning pursues a ''sum over states'' formulation in constructing the zeroth order Hamiltonian H_0 and the perturbation series. Different potentials may be invoked to construct H_0, and a wide range of potentials have been chosen[32,33] with varying degrees of success.

Besides the use of MR-MBPT in an incomplete model space, several other methods have been also proposed to overcome the convergence difficulties induced by the presence of intruder states. For example, the Murray–Davidson[34] approach defines the orbitals by diagonalizing the Fock operator F separately in the doubly occupied, singly occupied, and virtual spaces. The H_0 is then defined by using the resulting eigenvalues as orbital energies. Murray and Davidson also prescribe a second scheme in which the orbital energies are modified by adding a population dependent correction. The convergence behavior of the Murray–Davidson methods is similar to that for ROHF/UMP2 (restricted open shell Hartree–Fock/second order unrestricted Möller–Plesset theory). Roos and co-workers[35,36] use an alternative approach. The main disadvantage of the methods by Pulay[37] and Roos is that a very large set of linear equations must be solved. Hoffmann[38] obtains encouraging second order energies with scaled valence orbital energies for H_0, but the higher order convergence behavior is still unknown. Considerable theoretical and computational progress has appeared for the intermediate Hamiltonian method,[28] where the optimal zeroth order energies for the intermediate subspace are determined either by a judicious shifting[39–41] or by an iterative scheme.[42] This method introduces a shift operator to alter the eigenvalues of the intermediate space states, and it therefore appears that this shift operator enters into the third and higher orders, presumably pushing the divergence to higher orders. Moreover, a size-consistent intermediate-Hamiltonian formulation beyond second order is nontrivial.[43]

Freed and co-workers[44–52] have introduced a rather simple approach to tackle the intruder state problem. Their formulation is based on a Hermitianized version of Brandow's degenerate MR-MBPT theory in which V^{N-1} potentials are used for all valence orbitals and in which valence orbital degeneracy is imposed to enlarge the otherwise problematic perturbative energy denominators. The forced degeneracy condition, however, introduces an additional perturbation that enters beginning in third order, but the method significantly improves the perturbative convergence by removing serious intruder state problems. On the other hand, in the OPT method,[22,53] the perturbative convergence is accelerated by optimizing only a few zeroth order states. Our recent works on the HRS (rectangular H$_4$ system) and the Be atom demonstrate[22,53] how the forced valence orbital degeneracy approach (FD) and the OPT (optimized zeroth order energy) partitioning offer a decently convergent series (i.e., practical convergence) in situations where the traditional MP and EN multireference perturbative series are well known to be poorly divergent due to the presence of ''intruder'' states.

We have also demonstrated[22,53] the utility of two-state models as a diagnostic for understanding the perturbative convergence produced by various choices of reference spaces, partitioning methods, and orbitals, as well as in suggesting remedies for unsuitable choices. However, the analysis in these two studies is based on using a double reference space, which is the minimum size to qualify as a MR-MBPT computation. On the other hand, the FD partitioning scheme is generally applied with much larger reference spaces whose greater size ($\leqslant 5,000$ configuration state functions) might be thought to be more susceptible to intruder states that affect the perturbative convergence. The reference space in the FD partitioning is chosen, in part, based on a trade-off between generating accurate first order energies (and hence smaller perturbation corrections) from the enlarged reference space
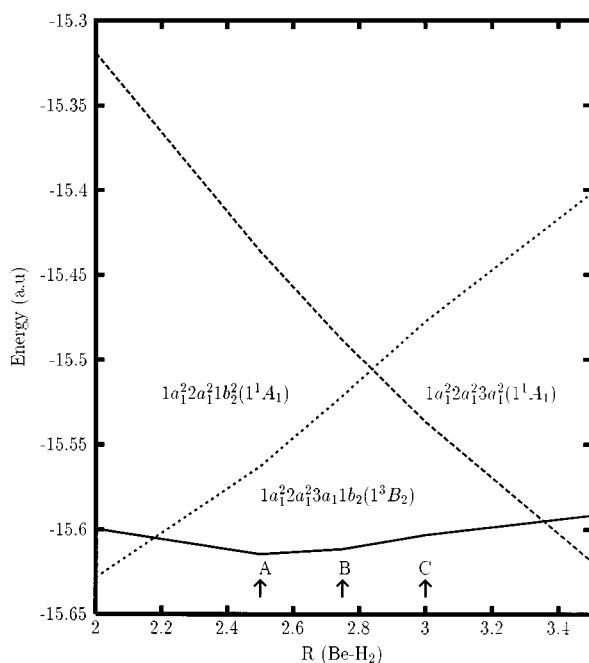
FIG. 1. SCF energies of BeH$_2$ for different ground state configurations and symmetries at various geometries along the reaction path.

at the expense of factors[22] that may slow or destroy the perturbative convergence, including the introduction of a large additional perturbation and the possible occurrence of small energy denominators from forcing the valence orbitals to be degenerate.[52] The present paper addresses the pessimistic view that the large reference space ultimately must degrade the convergence properties.

We consider the well-known difficult case of the excited $^1A_1$ state potential energy surface for the perpendicular C_{2v} insertion of Be (^1S) into H$_2$ (X$^1\Sigma_g^+$). This system has been investigated by Bartlett et al.,[54–56] Simons et al.,[57] Freed and co-workers,[58] and many other groups. The computations model the insertion path as a straight line $r = 2.54 - 0.46R$ (a.u.), where r is the H–H distance and R is the Be to center of H$_2$ distance. The treatment of this model reaction path is quite complicated due to the multiconfigurational nature of the electronic wave functions in certain regions. Purvis et al.[55] have shown that the perpendicular insertion of Be into H$_2$ requires p–orbital participation on Be and, in particular, the promotion of Be($2s^2$) to Be($2p^2$) near the critical geometry B for R=2.75 a.u. (see Fig. 1) due to the quasidegenerate nature of the 2s and 2p Be orbitals. This $2s \rightarrow 2p$ promotion changes the principal $^1A_1$ configuration along the BeH$_2$ reaction path from $1a_1^2 2a_1^2 3a_1^2$ to $1a_1^2 2a_1^2 1b_2^2$ as illustrated in Fig. 1. Thus at the critical or "transition" geometry B, the "excited" configuration $1a_1^2 2a_1^2 1b_2^2$ contributes more than the "ground" configuration $1a_1^2 2a_1^2 3a_1^2$ to the 1^1A_1 state (using SCF orbitals from the $1a_1^2 2a_1^2 1b_2^2$ state). A single reference perturbative model must treat one of these two important and strongly coupled configuration state functions (CSF) as lying in the orthogonal (Q) space (also called the virtual space), creating severe

convergence problems. When Be is moved to R=3.0 a.u. from the center of H$_2$ (geometry C), the 1^1A_1 state is dominated by the configuration $1a_1^2 2a_1^2 3a_1^2$, while at geometry A for R=2.5 a.u. (indicated on Fig. 1), the configuration $1a_1^2 2a_1^2 1b_2^2$ dominates over $1a_1^2 2a_1^2 3a_1^2$. A similar multiconfigurational character also appears in the H$_4$ model, where at the square planar geometry (i.e., when the separation R between the two H_2 fragments is 2.0 a.u.) the $a_{1g}^2 b_{1u}^2$ and $a_{1g}^2 b_{3u}^2$ CSFs are equally important for the 1^1A_{1g} state, but as the separation between the two H$_2$ fragments decreases (increases) the $a_{1g}^2 b_{3u}^2$ ($a_{1g}^2 b_{1u}^2$) CSF contributes significantly. The BeH$_2$ case is further complicated because the $1a_1^2 2a_1^2 3a_1 4a_1$ and $1a_1^2 2a_1^2 1b_2 2b_2$ CSFs are also very important. Thus, the complete study of the BeH$_2$ system is non-trivial even for describing one molecular potential energy surface.

Purvis et al.[55] have successfully described the 1^1A_1 state BeH$_2$ potential energy surface using different single configuration functions for different ranges of R in coupled cluster single and doubles (CCSD) calculations, but this approach may yield bumpy potential energy surfaces. Subsequently, Bartlett et al.[56] note that the choice of SCF orbitals from a $1a_1^2 2a_1^2 3a_1^1 1b_2^1$ ($^3B_2$) reference configuration provides a converged solution for the double reference MBPT (in which the $1a_1^2 2a_1^2 3a_1^2$ and $1a_1^2 2a_1^2 1b_2^2$ CSFs are chosen as the reference space) at the A, B, and C geometries. However, they fail to explain why the double reference MBPT converges at all three geometries only for the $^3B_2$ reference SCF orbital choice, an explanation that may aid in guiding further choice of molecular orbitals.

The present work analyzes the convergence problems encountered with MP and EN partitioning for double reference MBPT computations based on the $1a_1^2 2a_1^2 3a_1^2$ ($^1A_1$) state SCF orbitals and orbital energies. We demonstrate that converged solutions may still be obtained for all the three geometries using the same reference configuration $1a_1^2 2a_1^2 3a_1^2$ ($^1A_1$) SCF orbitals by (1) optimizing the zeroth order state energies, i.e, by employing our OPT method,[22,53], or (2) by applying the forced degeneracy (FD) partitioning scheme. Both methods use a more sensible selection of valence orbitals to enhance the perturbative convergence in low orders. Interestingly, recent computations for cis–butadiene (third order MR-MBPT) and for CH$_2$ by Freed and co-workers[59,60] also demonstrate the same trends.

Sections II and III briefly outline the multireference configuration perturbation theory and the choice of the zeroth order Hamiltonian. Section IV describes the convergence criteria for the perturbation expansion of a simple two-state model that is used in later sections to explain the behavior of the perturbation expansion with the full 197 state computation. Section V presents information concerning the basis set and the reference spaces used. Section VI describes why certain partitioning schemes yield convergence problems. The source of these convergence problems is analyzed using two-state models constructed from the full problem by selecting one important state each from the reference and orthogonal space states (called an interspace pair of states). Sections VII and VIII summarize the results of the OPT and FD partition-

ing with larger reference spaces and provide comparisons with other methods that have been used to compute the $1\,^1A_1 \rightarrow 2\,^1A_1$ vertical excitation energies of BeH$_2$.

II. BASIC FORMALISM OF MULTIREFERENCE MANY-BODY PERTURBATION THEORY (MR-MBPT)

The exact Hamiltonian is first partitioned into

$$H = H_0 + V, \tag{2.1}$$

where H_0 is the unperturbed Hamiltonian and V is the perturbation. We assume that the Schrödinger equation for the unperturbed Hamiltonian,

$$H_0|\Phi_i\rangle = E_i^0|\Phi_i\rangle, \tag{2.2}$$

provides a complete set of eigenfunctions $|\Phi_i\rangle$ with corresponding eigenvalues E_i^0. The eigenfunctions of H_0 are then divided into two subspaces defined by the two complementary projectors P and Q, where

$$P = \sum_i^d |\Phi_i\rangle\langle\Phi_i| = \sum_i P_i, \tag{2.3}$$

and

$$Q = 1 - P = \sum_{j=d+1} |\Phi_j\rangle\langle\Phi_j| = \sum_j Q_j. \tag{2.4}$$

The P subspace of dimension d is variously called the model, the reference, or the valence space, while its orthogonal complement Q is formed by the remaining eigenvectors of H_0. The model space functions $|\Psi_i^0\rangle$ are defined as the projections of the exact eigenfunctions $|\Psi_i\rangle$ onto the reference or model space,

$$|\Psi_i^0\rangle = P|\Psi_i\rangle. \tag{2.5}$$

Alternatively, the exact eigenfunctions $|\Psi_i\rangle$ can be reproduced from the model space function $|\Psi_i^0\rangle$ with the aid of the wave operator Ω,

$$|\Psi_k\rangle = \Omega|\Psi_k^0\rangle. \tag{2.6}$$

Using these definition of P, Q, and Ω, the exact and the perturbed Schrödinger equations may be cast into effective eigenvalue equations of the form

$$H_{\text{eff}}|\Psi_i^0\rangle = E_i|\Psi_i^0\rangle, \tag{2.7}$$

where H_{eff} is given by

$$H_{\text{eff}} = PH\Omega P. \tag{2.8}$$

An order-by-order perturbation expansion of Ω is obtained by solving the generalized Bloch equation[13,14]

$$[\Omega, H_0]P = [V\Omega - \Omega V\Omega]P. \tag{2.9}$$

Now define the perturbative expansion of the wave operator Ω as

$$\Omega = 1 + \Omega^{(1)} + \Omega^{(2)} \cdots. \tag{2.10}$$

Substituting the expansion for Ω into Eq. (2.9) generates the nth order expression for Ω as

$$[\Omega^{(n)}, H_0]P = \left[V\Omega^{(n-1)} - \sum_{m=1}^{n-1} \Omega^{(m)} V\Omega^{(n-m-1)}\right]P, \tag{2.11}$$

and the corresponding matrix elements of the nth order contribution to H_{eff} are given by

$$\langle\Phi_i^0|H_{\text{eff}}^{(n)}|\Phi_j^0\rangle = \langle\Phi_i^0|PV\Omega^{(n-1)}P|\Phi_j^0\rangle. \tag{2.12}$$

The expressions for the effective Hamiltonian matrix elements through third order is then obtained as

$$\begin{aligned}
\langle\alpha|H_{\text{eff}}^{(1\rightarrow3)}|\beta\rangle &= E_\alpha^0\delta_{\alpha\beta} + \langle\alpha|V|\beta\rangle \\
&+ \sum_{m\in Q} \frac{\langle\alpha|V|m\rangle\langle m|V|\beta\rangle}{E_\beta^{(0)} - E_m^{(0)}} \\
&+ \sum_{m,n\in Q} \frac{\langle\alpha|V|m\rangle\langle m|V|n\rangle\langle n|V|\beta\rangle}{(E_\beta^{(0)} - E_m^{(0)})(E_\beta^{(0)} - E_n^{(0)})} \\
&- \sum_{m\in Q, \gamma\in P} \frac{\langle\alpha|V|m\rangle\langle m|V|\gamma\rangle\langle\gamma|V|\beta\rangle}{(E_\beta^{(0)} - E_m^{(0)})(E_\gamma^{(0)} - E_m^{(0)})}.
\end{aligned} \tag{2.13}$$

The above effective Hamiltonian H_{eff} in Eq. (2.13) is non-Hermitian as is evident from the antisymmetry of its energy denominators. Introducing a Hermitized form of Ω enables generating a Hermitian H_{eff}[11,13], which through third order is equivalent to using $\frac{1}{2}(H_{\text{eff}} + H_{\text{eff}}^\dagger)$. Provided the dimension of the Q space is not very large, the order by order computation of H_{eff} from Eq. (2.11) is relatively straightforward and is performed in this present work.

Although not explicitly indicated in the above equations, the wave operator Ω introduced here actually depends upon the model function on which it operates, i.e., is a state or ket dependent wave operator. Further, the above derivation of H_{eff} assumes that Ω satisfies intermediate normalization (i.e., $P\Omega P = P$), which, in fact, is not mandatory.[26]

III. CHOICES OF ZEROTH ORDER HAMILTONIAN H_0

The choice of the zeroth order Hamiltonian is, *in principle*, at our disposal. However, the choice, *in practice*, strongly determines the convergence properties of the perturbative expansion. Several types of zeroth order Hamiltonians H_0 are considered here.

A. Möller–Plesset (MP) partitioning

The MP partitioning uses a ''sum over orbitals'' form of H_0. The most general diagonal form of such a H_0 is given by

$$H_0 = \sum_c^{N_c} \epsilon_i a_c^\dagger a_c + \sum_v^{N_v} \epsilon_v a_v^\dagger a_v + \sum_e^{N_c} \epsilon_e a_e^\dagger a_e, \tag{3.1}$$

where N_c, N_v, and N_e are the numbers of core, valence, and excited orbitals, ϵ_c, ϵ_v, and ϵ_e are the corresponding orbital energies, and $a_i^\dagger$ and a_i are the usual creation and annihilation operators, respectively. The orbitals are usually defined as eigenfunctions of Fock operators. The most natural choice for the orbital energies ϵ_i are the eigenvalues of the Fock operator defining the orbitals. However, any choice of orbit-

als and orbital energies may, in principle, be chosen, and the objective is to find choices that assure the most rapid perturbative convergence. Traditional MP partitioning, on the other hand, defines all orbitals and orbital energies as the eigenfunctions and eigenvalues of a *single* Fock operator, a choice that has proven to be quite useful for SR-MBPT computations but that is not designed towards optimal perturbative convergence of the multireference extensions.[61]

B. Forced valence orbital degenerate (FD) partitioning

This method is a variant of the general MP partitioning method as embodied in Eq. (3.1). However, in order to improve the perturbative convergence and to remove the serious intruder state problems, Freed and co-workers use multiple Fock operators to obtain the spatial orbitals.[47,49,52] The valence orbitals and orbital energies are obtained using $V^{(N-1)}$ potentials,[47,49,52] and the valence orbital energies are then forced to be degenerate. The form of the diagonal H_0 in the FD partitioning is given by

$$H_0 = \sum_c^{N_c} \epsilon_c a_c^\dagger a_c + \bar{\epsilon}_v \sum_v^{N_v} a_v^\dagger a_v + \sum_e^{N_e} \epsilon_e a_e^\dagger a_e, \qquad (3.2)$$

where the average valence orbital energy $\bar{\epsilon}_v$ is obtained from the original set of valence orbital energies by the democratic averaging

$$\bar{\epsilon}_v = \frac{\sum_i^{N_v} \epsilon_v}{N_v}. \qquad (3.3)$$

The above degeneracy condition introduces a diagonal perturbation $\delta V = \epsilon_v - \bar{\epsilon}_v$ that contributes beginning in third order. The magnitude of δV directly depends upon of the spread of the original valence orbital energies $\{\epsilon_v\}$ before averaging. In fact, some third order computations with small, quasidegenerate reference spaces do not require valence orbital energy averaging.

C. Epstein–Nesbet (EN) partitioning

The most general diagonal form of H_0 can be written as

$$H_0 = \sum_i |i\rangle E_i^0 \langle i|, \qquad (3.4)$$

where the sum over i runs over all states and E_i^0 is the ith state zeroth order energy, which is formally at our disposal. Usually, Epstein–Nesbet partitioning chooses the zeroth order state energy as

$$E_i^0 = \langle i|H|i\rangle, \qquad (3.5)$$

which makes the diagonal elements of V vanish with either a determinantal or CSF basis. Since the H_0 differs for the latter two cases, the determinantal–based Epstein–Nesbet and CSF-based Epstein–Nesbet partitioning methods generate different perturbation expansions. (Note that a unitary transformation of the H_0 from a determinantal-based Epstein–Nesbet basis to a CSF basis leads to a nondiagonal H_0.) The computation below, denoted by EN, employs a hybrid of the determinantal and CSF-based Epstein–Nesbet partitionings.

This variant of Epstein–Nesbet partitioning defines the zeroth-order energies of each CSF by the barycentric expression,[62]

$$E_i^0 = \sum_d [C_d^i]^2 \langle d|H|d\rangle, \qquad (3.6)$$

where the CSF function $|i\rangle$ is given by a linear combination of determinantal states $|d\rangle$,

$$|i\rangle = \sum_d C_d^i |d\rangle. \qquad (3.7)$$

Our previous investigation of the HRS and the Be atom[22,53] also employs this partitioning method. Except for single determinantal states $|i\rangle$, the diagonal matrix elements of the perturbation V no longer vanish for the EN H_0 of Eqs. (3.6) and (3.7).

D. Optimized zeroth order (OPT) partitioning

The optimized zeroth order partitioning (OPT) approach applied here is similar to the EN partitioning method in using a H_0 of the form in Eq. (3.5), but the OPT method differs significantly because a small subset of the zeroth order state energies E_i^0 are determined in an optimal manner.[22,53] The ''optimal performance'' of the perturbation expansion is defined as follows: The state energies of the lowest 20 BeH$_2$ zeroth order states are selected to optimize the low order convergence of the perturbative expansion. The process minimizes the sum of the absolute deviations of the perturbative energies through third and fourth orders from the infinite order (converged) FCI (full configuration interaction) ground state energy E_{gs} as calculated *within* the subspace of the same twenty lowest zeroth order states. More precisely, the OPT partitioning involves minimizing the sum of the third and fourth order absolute deviations,

$$|E_{gs} - E_3| + |E_{gs} - E_4|, \qquad (3.8)$$

where E_3 and E_4 are the third and fourth order perturbation computations of E_{gs} as obtained using the same 20 zeroth order states. Since Eq. (3.4) is invariant to a constant shift of all twenty zeroth order state energies, for convenience, we select the ground state zeroth order energy to be fixed at its barycentric EN value. The state energies for all the remaining Q-space CSFs are also fixed at their barycentric EN state energies. Thus, the form of H_0 in this partitioning scheme is written as

$$H_0 = \sum_i |i\rangle \bar{E}_i^0 \langle i|,$$

where $\bar{E}_i^0$ is the optimal zeroth order energy of state $|i\rangle$ for the lowest 20 states, while the remainder are EN barycenter values.

IV. TWO STATE SYSTEMS AS AN IMPORTANT DIAGNOSTIC

The convergence properties for the BeH$_2$ computations are explained transparently in subsequent sections by the use

of simple two-dimensional models that are constructed from a pair of interspace states, defined as one state each from the P and Q spaces, taken from the full problem with 197 CSFs. The convergence behavior is investigated by considering the parameterized Hamiltonian $H(z)$,

$$H(z) = H_0 + zV, \tag{4.1}$$

where z is the complex perturbation parameter. The $z=1$ limit recovers the exact two state H, while $z=0$ produces the unperturbed systems. Denote $|p\rangle$ and $|q\rangle$ as the P and Q space states of the two-dimensional model, while ϵ_p and ϵ_q are their zeroth order energies, respectively. The exact eigenvalues of the two-dimensional Hamiltonian $H(z)$ can be expressed as

$$E_\pm(z)$$
$$= \tfrac{1}{2}\ \text{Tr } \mathbf{H} \pm \tfrac{1}{2}\{[\Delta\epsilon - (\Delta\epsilon - \Delta H)z]^2 + 4V_{pq}^2 z^2\}^{1/2}, \tag{4.2}$$

where

$$V_{pq} = \langle p|H(z=1)|q\rangle,$$
$$\Delta\epsilon = \epsilon_q - \epsilon_p,$$
$$\Delta H = \langle q|H(z=1)|q\rangle - \langle p|H(z=1)|p\rangle,$$

and the z dependent trace of the Hamiltonian matrix $\mathbf{H}$ is given by

$$\text{Tr } \mathbf{H} = \langle p|H(z)|p\rangle + \langle q|H(z)|q\rangle.$$

Both eigenvalues become degenerate in the complex z-plane at the pair of branch points z_d and z_d^* where use of Eq. (4.2) gives

$$z_d = \frac{\Delta\epsilon}{4V_{pq}^2 + (\Delta\epsilon - \Delta H)^2}[(\Delta\epsilon - \Delta H) + 2V_{pq}i]. \tag{4.3}$$

The radius of convergence R_c for the single reference two state Rayleigh–Schrödinger perturbation expansion is $R_c = |z_d| = |z_d^*|$ and follows from Eq. (4.3) as

$$R_c = \sqrt{\frac{(\Delta\epsilon)^2}{(\Delta\epsilon - \Delta H)^2 + 4V_{pq}^2}}. \tag{4.4}$$

To achieve a convergent perturbation series, it is necessary to have $R_c \geq 1$, which occurs only if the numerator in Eq. (4.4) exceeds the denominator. This condition for convergence implies that $\Delta\epsilon$ (the zeroth order energy difference) must satisfy the requirements

$$\Delta\epsilon \begin{cases} \geq \dfrac{1}{2}\left[\Delta H + \dfrac{4V_{pq}^2}{\Delta H}\right] & \text{if } \Delta H > 0, \\[2mm] \leq \dfrac{1}{2}\left[\Delta H + \dfrac{4V_{pq}^2}{\Delta H}\right] & \text{if } \Delta H < 0 \end{cases}. \tag{4.5}$$

Thus both $\Delta\epsilon$ and ΔH must have the same sign; otherwise the two-state perturbation series diverges. Also, when $\Delta H \neq 0$, Eq. (4.5) indicates that $\Delta\epsilon$ can always be selected so that $R_c > 1$. Wilson et al. arrive at the same conclusion by examining the maximum radius of convergence R_c as a function of $\Delta\epsilon$.[63] Note that the features exhibited by Eqs. (4.3)–(4.5) are also displayed by the general behavior of the full

197 CSF BeH$_2$ computations that follow. This behavior is modeled in Sec. V by selecting the most influential pairs of interspace states and by analyzing the character of the full computation for $z \approx z_d$. Thus, two state interspace models provide both convergence criteria and a useful diagnostic tool for assessing the probable perturbative behavior of various MR partitioning methods.

Intruder states are defined as the orthogonal (Q) space states responsible for destroying the convergence of a perturbation expansion. The presence of intruder states is usually detected by observing the variation of the eigenvalues as a function the of perturbation parameter z for real z. An avoided crossing occurs at a point z_{ac} where the two eigenvalues are closest. The avoided crossing is computed in the two state model by minimizing $[E_-(z) - E_+(z)]$ with respect to Re z_d,

$$z_{ac} = \frac{\Delta\epsilon(\Delta\epsilon - \Delta H)}{4V_{pq}^2 + (\Delta\epsilon - \Delta H)^2}. \tag{4.6}$$

Comparing Eqs. (4.3) and (4.6) shows that z_{ac} is simply Re z_d. [Note that the eigenvalues $E_-(z)$ and $E_+(z)$ cannot be degenerate for real z.] If the avoided crossing appears for $0 < z_{ac} < 1$, the perturbation expansion diverges ($R_c < 1$), and the convergence is disrupted by what is termed a ''front door'' intruder state. Similarly, an avoided crossing for $z_{ac} < 0$ is called a backdoor intruder state[64,65] when $R_c < 1$. Equation (4.5) implies that a backdoor intruder state $z_{ac} < 0$ occurs whenever ΔH and $\Delta\epsilon$ have the same signs and satisfy $|\Delta H| > |\Delta\epsilon|$. On the other hand, if $\Delta\epsilon$ and ΔH are of opposite signs (called incorrect energy ordering) or if $|\Delta H| < |\Delta\epsilon|$, then the avoided crossing appears for $z_{ac} > 0$.

When incorrect energy ordering is present in the two state system, the expansion is always divergent ($R_c < 1$). Also, with incorrect ordering present, the limit of $V \rightarrow 0$ has Im $z \rightarrow 0$, and z_d is real and positive with

$$z_d \rightarrow \frac{\Delta\epsilon}{(\Delta\epsilon - \Delta H)}. \tag{4.7}$$

Equation (4.7) also emerges when the z-dependent diagonal elements of H are degenerate. Thus in actual calculations involving a large number of states, if the incorrectly ordered pair of interspace states is weakly coupled both among themselves and to other states, then both z_d and z_{ac} are approximately equal to the value of z where the diagonal elements of $H(z)$ are degenerate. Furthermore, such cases yield a very pronounced avoided crossing since the degeneracy point z_d occurs close to the real axis. This situation is found in Sec. V for the FD partitioning computations with a three-orbital reference space. By contrast, when a two-state system has the zeroth order states correctly ordered, the limit of $V \rightarrow 0$ then produces $R_c \rightarrow \infty$ corresponding to a convergent expansion. In addition, the special case of $\Delta H = \Delta\epsilon$ (standard Epstein–Nesbet partitioning for a determinantal or CSF basis) yields the avoided crossing at $z_{ac} = 0$ since Eq. (4.3) implies that this case produces z_d as purely imaginary.

It should be emphasized that, in general, for large scale MBPT computations, we often neither know nor care

whether the perturbation series converges, since this information has little practical value for computations truncated at low orders except to guide the development of improved low order methods. However, this convergence behavior has bearing on infinite order methods such as coupled-cluster (CC) approaches. Mathematical convergence depends upon the behavior of the indefinitely high order terms, whereas low order truncations are often very accurately provided by formally divergent asymptotic series. For example, many formally divergent series are asymptotically convergent and are quite useful when truncated at low orders [e.g., Stirling's formulas for the expansion of $\ln n!$ and $\sin(2\epsilon)$]. Thus, when divergent series are obtained from the full scale calculations, these series are analyzed below to assess their useful asymptotic character and their behavior when resumed by Padé approximants.

V. BASIS SET AND REFERENCE SPACE

We employ a contracted [12s3p/3s1p] set of Gaussian functions for Be and [4s/2s] contracted Gaussian functions (with scaling factor of 1.2) for the H atoms. This basis is the same as applied by Purvis and Bartlett in their ground state computation for BeH₂.[55] Ground state SCF calculations produce the minimum energy state as a $1a_1^2 2a_1^2 3a_1^1 1b_2^1 \ ^3B_2$ state for all the geometries considered here. The next two low lying states have the configurations (symmetries) of $1a_1^2 2a_1^2 3a_1^2 \ (^1A_1)$ and $1a_1^2 2a_1^2 1b_2^2 \ (^1A_1)$ and cross near geometry B (see Fig. 1). Our first model space for all the geometries contains the two zeroth order $1a_1^2 2a_1^2 3a_1^2$ and $1a_1^2 2a_1^2 1b_2^2$ states. This double reference space is used to study the convergence behavior for the two lowest $^1A_1$ excited states with all four different partitioning schemes, the MP, EN, FD, and OPT partitionings. The double reference space calculation for the states of $^1A_1$ symmetry yields a Q-space with 195 states since the $1a_1$ orbital is kept doubly occupied in all the CSFs (frozen core). We compute through 30th order the order-by-order state energies and vertical excitation energy for the $1\ ^1A_1 \rightarrow 2\ ^1A_1$ transition using the configuration based MR-MBPT algorithm.[55] Excitation energies for all reference spaces are taken relative to the $1\ ^1A_1$ state, although the $^3B_2$ state is the lowest lying SCF state. We also compute the order by order state energies using FD partitioning with larger reference spaces (described below) in order to analyze how the convergence behavior is affected by enlarging the reference space. Since increasing the size of the reference space enhances some diagonal perturbation matrix elements (due to the reduced quasidegeneracy among the valence orbitals) and may introduce energy denominators that are too small,[52] it might be expected that the perturbation series diverges more quickly with the larger than the smaller reference spaces. On the other hand, the larger reference space provides improved first order energies [from the first two terms on the right hand side of Eq. (2.13)] and smaller overall perturbation corrections [from the Q space contributions in Eq. (2.13)]. The question we address with the larger reference spaces is which of these competing factors domi-

nates when larger reference space computations are truncated at low (e.g., third) orders. (Other factors influencing convergence are discussed in Ref. 22).

While the FD and traditional MP partitioning approaches both begin from the same form of the zeroth order Hamiltonian [Eq. (3.2)], both the orbitals and orbital energies are chosen quite differently with the FD partitioning scheme than with conventional MP methods. We illustrate these differences using the double reference space FD-MBPT computation with the $1a_1^2 2a_1^2 3a_1^2$ and $1a_1^2 2a_1^2 1b_2^2$ CSFs as the reference space. The $1a_1$, $2a_1$, and $3a_1$ orbitals and orbital energies are first obtained from a closed shell SCF computation for the $1a_1^2 2a_1^2 3a_1^2$ state. The $1b_2$ unoccupied valence orbital and orbital energy are then computed as the improved virtual orbital (IVO) from a $1a_1^2 2a_1^2 3a_1^1 1b_2^1$ state SCF in which only the $1b_2$ is permitted to vary.[47,49,52] This procedure yields a $1b_2$ orbital that is more suited to describe excited states than the virtual $1b_2$ orbital from the $1a_1^2 2a_1^2 3a_1^2$ state SCF, and the $1b_2$ orbital energy is lower than that of the virtual $1b_2$ orbital, making the FD reference space more quasidegenerate than the conventional MP choice. The FD partitioning excited orbitals and orbital energies are then obtained by diagonalizing the $1a_1^2 2a_1^2 3a_1^2$ state Fock operator with the core and valence orbitals frozen. The $3a_1$ and $1b_2$ orbital energies are then replaced by their arithmetic average to impose degeneracy on the reference space and thereby to eliminate the worst intruder state problems. All OPT computations use the same orbitals as for the double reference FD treatments but optimize the zeroth order energies.

The FD computations with the larger reference spaces begin with the three SCF a_1 symmetry orbitals that are occupied in the Hartree–Fock (HF) $1\ ^1A_1$ state. The $1a_1$ orbital is placed in the core, while the $2a_1$ and $3a_1$ orbitals are valence orbitals. (The five valence orbital reference space leaves the $2a_1$ orbital in the core). Additional valence orbitals (of symmetries a_1, b_2 and b_1) that are unoccupied in the HF $1\ ^1A_1$ state are taken to be improved virtual orbitals (IVOs) created by a single SCF optimization for an excited triplet configuration in which an electron is promoted from the highest occupied molecular orbital (the HOMO in the $1\ ^1A_1$ HF state) into the orbital to be optimized. The procedure for obtaining the molecular orbitals involves a sequence of SCF calculations (which can also be obtained by a unitary transformation[52]). For example, the four orbital reference space is produced by the sequence,

(1) $\qquad 1a_1^2 2a_1^2 3a_1^2$, $\qquad\qquad\qquad ^1A_1$,

(2) $\qquad [1a_1^2 2a_1^2 3a_1^1]1b_2^1$, $\qquad\qquad ^3B_2$,

(3) $\qquad [1a_1^2 2a_1^2 3a_1^1 1b_2^0]1b_1^1$, $\qquad ^3B_1$,

(4) $\qquad [1a_1^2 2a_1^2 3a_1^1 1b_2^0 1b_1^0]4a_1^1$, $\qquad ^3A_1$.

The first step is a $1\ ^1A_1$ state SCF calculation, and steps 2–4 are independent single orbital optimization, where the orbitals shown in the square brackets are frozen as determined in the previous steps. The excited orbitals are then obtained by diagonalizing the $1\ ^1A_1$ state Fock operator in the orbital

TABLE I. Energy errors $|E_{FCI} - E(N)|$ for the first $(1\ ^1A_1)$ and second $(2\ ^1A_1)$ BeH$_2$ $^1A_1$ states at geometry A for different partitioning schemes and a double reference space.

Perturbation order (N)	MP	EN	FD	OPT
1 $^1A_1$				
2	0.009 797	0.157 627	0.031 318	0.018 660
3	0.016 333	0.039 239	0.003 538	0.003 447
4	0.004 052	0.095 676	0.007 560	0.002 372
5	0.008 312	0.392 442	0.002 525	0.003 765
6	0.006 090	0.579 366	0.001 381	0.001 823
7	0.002 344	0.107 665	0.001 914	0.000 082
8	0.004 946	0.145 447	0.000 670	0.000 637
9	0.000 629	Diverges	0.000 410	0.000 419
10	0.003 207		0.000 597	0.000 083
20	0.001 192		0.000 015	0.000 005
30	0.000 602		0.000 000	0.000 000
2 $^1A_1$				
2	0.038 894	0.016 427	0.033 002	0.000 516
3	0.018 555	0.000 012	0.014 819	0.002 580
4	0.009 554	0.192 088	0.008 113	0.000 849
5	0.005 216	0.000 126	0.004 879	0.000 370
6	0.002 602	0.007 227	0.002 959	0.000 320
7	0.001 096	Diverges	0.001 750	0.000 053
8	0.000 464		0.001 009	0.000 017
9	0.000 290		0.000 568	0.000 023
10	0.000 190		0.000 309	0.000 014
20	0.000 030		0.000 008	0.000 006
30	0.000 014		0.000 000	0.000 000

TABLE II. Energy errors $|E_{FCI} - E(N)|$ for the first $(1\ ^1A_1)$ and second $(2\ ^1A_1)$ BeH$_2$ $^1A_1$ states at geometry B for different partitioning schemes and a double reference space.

Perturbation order (N)	MP	EN	FD	OPT
1 $^1A_1$				
2	0.006 905	0.229 169	0.031 095	0.022 453
3	0.020 273	0.033 213	0.001 843	0.003 807
4	0.003 027	0.029 801	0.005 811	0.001 704
5	0.014 420	1.54 592	0.000 988	0.001 939
6	0.005 827	Diverges	0.002 114	0.001 327
7	0.012 646		0.001 994	0.000 581
8	0.010 047		0.000 498	0.000 155
9	0.006 871		0.000 558	0.000 058
10	0.010 741		0.000 601	0.000 054
20	0.000 183		0.000 004	0.000 004
30	0.100 391		0.000 003	0.000 000
	Diverges			
2 $^1A_1$				
2	0.025 440	0.026 385	0.032 683	0.008 274
3	0.006 805	0.082 865	0.009 783	0.004 344
4	0.006 542	0.698 845	0.003 550	0.005 356
5	0.013 767	0.017 071	0.002 335	0.002 886
6	0.003 736	0.025 721	0.002 347	0.000 471
7	0.004 565	Diverges	0.001 767	0.000 252
8	0.003 360		0.000 757	0.000 208
9	0.005 668		0.000 031	0.000 136
10	0.008 212		0.000 181	0.000 092
20	0.000 210		0.000 003	0.000 001
30	0.012 616		0.000 001	0.000 000
	Diverges			

space complementary to the union of the core and reference spaces. This four orbital reference space is denoted symbolically as $(\text{core})^2[2a_1 3a_1 1b_1 1b_2]^4$ to indicate the valence orbitals in square brackets and the total number of electrons in the reference space as the superscript. The corresponding six and seven orbital reference spaces are $(\text{core})^2[2a_1 3a_1 1b_1 1b_2 2b_2]^4$, and $(\text{core})^2[2a_1 3a_1 4a_1 1b_1 1b_2 2b_2]^4$, respectively.

VI. CONVERGENCE PROBLEM FOR BeH$_2$ WITH DIFFERENT PARTITIONING SCHEMES

A. Convergence difficulties with Möller–Plesset (MP) and Epstein–Nesbet (EN) partitioning schemes using a double reference space

The computations in this section employ a reference space with the $|1a_1^2 2a_1^2 3a_1^2\rangle$ and $|1a_1^2 2a_1^2 1b_2^2\rangle$ CSFs as the model or reference space states. Using this double reference space, the computed MR-MBPT energies for the lowest two $^1A_1$ states are displayed in Tables I, II, and III for geometries A, B, and C, respectively, and for the EN, MP, FD, and OPT partitioning schemes. The tables demonstrate the previously known fact[56] that the traditional MP and EN partitioning multireference perturbation expansions suffer from convergence problems for both $^1A_1$ states of BeH$_2$ and for all the geometries (except geometry A for MP). The analysis below demonstrates that the severe divergence encountered with the traditional MP and EN partitionings arises from the presence of intruder states that render these series divergent. Detailed analysis is presented for the "transition state" geometry B

TABLE III. Energy errors $|E_{FCI} - E(N)|$ for the first $(1\ ^1A_1)$ and second $(2\ ^1A_1)$ BeH$_2$ $^1A_1$ states at geometry C for different partitioning schemes and a double reference space.

| Perturbation	MP	EN	FD	OPT
1 $^1A_1$				
2	0.017 247	0.283 610	0.024 418	0.015 736
3	0.00 0707	0.012 123	0.005 582	0.005 203
4	0.010 640	0.010 601	0.002 057	0.000 446
5	0.012 240	Diverges	0.001 973	0.000 492
6	0.033 151		0.001 511	0.001 089
7	0.003 558		0.000 703	0.001 061
8	0.042 671		0.000 044	0.000 473
9	1.01 971		0.000 196	0.000 118
10	0.018 561		0.000 108	0.000 297
20	Diverges		0.000 011	0.000 002
30			0.000 000	0.000 010
2 $^1A_1$				
2	0.016 127	0.082 610	0.038 595	0.014 856
3	0.025 115	0.282 279	0.00 0071	0.002 385
4	0.048 321	1.715 727	0.005 922	0.003 227
5	0.001 993	Diverges	0.000 563	0.000 864
6	0.038 506		0.003 697	0.000 908
7	0.224 649		0.003 296	0.000 174
8	0.132 104		0.000 696	0.000 292
9	0.086 502		0.001 031	0.000 048
10	2.838 345		0.000 971	0.000 284
20	Diverges		0.000 033	0.000 112
30			0.000 014	0.000 005
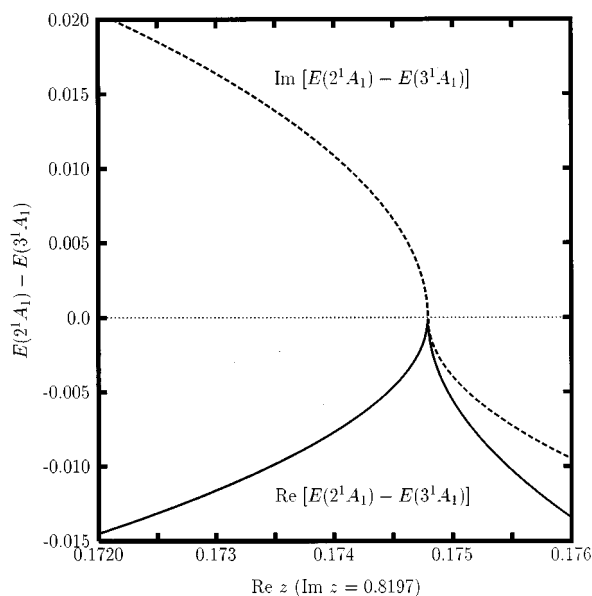
FIG. 2. z–dependent excitation energy $E(2^1A_1) - E(3^1A_1)$ of BeH₂ for geometry B from MP partitioning scheme.

only for convenience. The convergence difficulties at the other two geometries (as well as several others not discussed here) may be shown to occur for similar reasons.

We now examine the z-dependent FCI eigenvalues and eigenfunctions of the complex $H(z)$ of Eq. (4.1) from the MP and EN partitionings as a function of the perturbation parameter z. This analysis yields the radius of convergence $R_c = |z_d|$, where z_d is the closest degeneracy point to the origin involving two states that become an interspace pair of states as $z \rightarrow 0$. One of the two degenerate states at $z = z_d$ evolves into a P space state as $z \rightarrow 0$ (a P–corresponding state) and the other to a Q space state (a Q–corresponding state). The MP and EN partitionings with double reference spaces have no zeroth order energy overlap between the P and Q spaces. Thus the degeneracy point z_d defining R_c involves the $2\,^1A_1$ (P–corresponding) and $3\,^1A_1$ (Q–corresponding) states. The $2\,^1A_1$ state for the MP and EN partitionings evolves into the $|1a_1^2 2a_1^2 1b_2^2\rangle$ (P space) CSF when $z \rightarrow 0$, while the $3\,^1A_1$ state evolves into the $|1a_1^2 2a_1^2 3a_1^1 4a_1^1\rangle$ ($|1a_1^2 2a_1^2 1b_2^1 2b_2^1\rangle$) Q-space CSF for MP (EN) partitioning. The intruder state is defined as the *zeroth order state* from the Q space state that contributes most to the P–corresponding state in the vicinity of z_d. Other slightly different definitions of an intruder state have also been used. Schucan and Weidenmüller[20,21] identify the intruder states as problematic "collective states," composed predominantly of Q space states, that near $z = 1$ describe low lying exact states.

The MP partitioning z-dependent eigenvalue differences are depicted in Fig. 2 for the second and third states of $^1A_1$ symmetry for complex z, i.e., $E_{2^1A_1}(z) - E_{3^1A_1}(z)$. Figure 2 establishes the presence of a degeneracy between these two interspace $^1A_1$ states. Since the real and imaginary parts of the eigenvalues for the second (P–corresponding) and third

(Q–corresponding) states of $^1A_1$ symmetry are degenerate for $z_d \approx 0.17 \pm 0.82i$, the radius of convergence is $R_c = 0.84$ for the perturbation expansion. In the vicinity of z_d, the first excited state ($2\,^1A_1$) eigenfunction with MP partitioning is dominated by 48% of $|1a_1^2 2a_1^2 1b_2^2\rangle$ (P space) and 41% of $|1a_1^2 2a_1^2 1b_2 2b_2\rangle$ (Q space) CSFs, and the second excited state ($3\,^1A_1$) eigenfunction is described by the CSFs $|1a_1^2 2a_1^2 1b_2^2\rangle$ (43%) and $|1a_1^2 2a_1^2 1b_2 2b_2\rangle$ (48%). [For $z = 0$, the second excited state ($3\,^1A_1$) is, however, described by the CSF $|1a_1^2 2a_1^2 3a_1 4a_1\rangle$].

A two state model with the $|1a_1^2 2a_1^2 1b_2^2\rangle$ and $|1a_1^2 2a_1^2 1b_2 2b_2\rangle$ interspace pair of CSFs yields $z_d = 0.32 \pm 0.80i$, with $R_c = 0.86$ as the radius of convergence. Thus, we find semi-quantitative agreement between the estimate for the radius of convergence from the full computation and that from the two state model. The intruder state is identified in the full computation to be the $|1a_1^2 2a_1^2 1b_2 2b_2\rangle$ state, and divergence occurs because the $|1a_1^2 2a_1^2 1b_2^2\rangle$ and $|1a_1^2 2a_1^2 1b_2 2b_2\rangle$ interspace pair have too small a zeroth order energy difference [see Eq. (4.5)]. However, the zeroth order energy difference between this interspace pair is far from quasidegenerate. (Reference 53 provides a similar explanation for the divergent behavior of the MP partitioning series with four hydrogen atoms arranged in a rectangular.) Since the degeneracy occurs for $1 > \mathrm{Re}\, z_d > 0$, the $|1a_1^2 2a_1^2 1b_2 2b_2\rangle$ CSF may be characterized as a front-door intruder state. On the other hand, there is no avoided crossing visible on the real axis because z_d is far from the real axis. Hence, we prefer to characterize this intruder state as a "hidden" intruder state.

An avoided crossing is present between the second and third states of $^1A_1$ symmetry for barycentric–EN partitioning, but the states are so far apart that a plot of $E_m(z)$ vs $\mathrm{Re}\, z$ gives little hint of this crossing. However, allowing z to be complex, we find that the second and third $^1A_1$ states become degenerate (see Fig. 3) with $z_d \approx -0.06 \pm 0.28i$ ($R_c = 0.29$). Near z_d, the eigenfunction of the second $^1A_1$ state is dominated by 57% of $|1a_1^2 2a_1^2 1b_2^2\rangle$ (P space) and 31% of $|1a_1^2 2a_1^2 1b_2 2b_2\rangle$ (Q space) CSFs, whereas the eigenfunction of the third $^1A_1$ state is described by the CSFs $|1a_1^2 2a_1^2 1b_2^2\rangle$ (36%) and $|1a_1^2 2a_1^2 1b_2 2b_2\rangle$ (48%). A two state model with this interspace pair of CSFs yields the estimated radius of convergence as 0.35 from $z_d \approx -0.06 \pm 0.34i$, which compares quite favorably with the R_c from full 197 CSF calculation. Hence, as in MP partitioning, the $|1a_1^2 2a_1^2 1b_2 2b_2\rangle$ state is clearly the intruder state and divergence occurs because the $|1a_1^2 2a_1^2 1b_2^2\rangle$ and $|1a_1^2 2a_1^2 1b_2 2b_2\rangle$ interspace pair have too small a zeroth order energy difference [see Eq. (4.5)]. A similar explanation was also given for the divergent behavior of barycentric–EN partitioning with four hydrogen atoms arranged in a rectangle.[53]

Both the MP and EN partitionings obtain their SCF orbitals from the $|1a_1^2 2a_1^2 3a_1^2\rangle$ state. This arbitrary choice leaves the $|1a_1^2 2a_1^2 1b_2^2\rangle$ and $|1a_1^2 2a_1^2 1b_2 2b_2\rangle$ interspace pair strongly coupled, which, in part, produces divergent expansions for both partitionings. If instead, the orbitals are obtained from the $|1a_1^2 2a_1^2 1b_2^2\rangle$ state, then, Brillouin's theo-
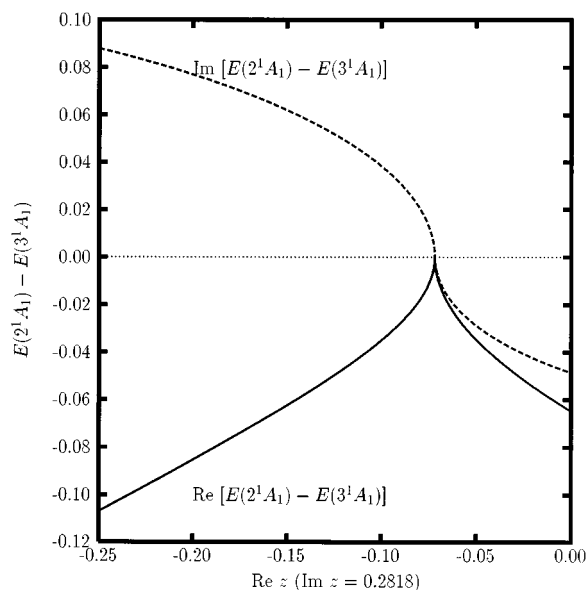
FIG. 3. z-dependent excitation energy $E(2\,^1A_1)-E(3\,^1A_1)$ of BeH₂ for geometry B from barycentric–EN partitioning scheme.

TABLE IV. Energy errors $|E_{\text{FCI}}-E(N)|$ for the ground state $(1\,^1A_1)$ of BeH₂ at geometry B as obtained from FD-series (for five valence orbital reference space) through [N,M] Padé resummation.

Order	FD-series	[N,M]th order Padé	
2	0.003 251 59		
3	0.008 871 37	[1,0]	−0.003 405 97
4	−0.007 048 93	[1,1]	0.000 684 01
5	0.000 707 79	[2,1]	0.000 058 05
6	−0.010 484 78	[2,2]	0.000 011 97
7	0.003 333 65	[3,2]	−0.000 041 00
8	−0.022 805 16	[3,3]	−0.000 005 09
9	−0.149 567 97	[4,3]	−0.000 005 09
10	−1.415 019 25	[4,4]	−0.000 005 10
11	−2.591 356 20	[5,4]	−0.000 004 60
12	−8.714 815 07	[5,5]	−0.000 004 74
13	−14.429 572 62	[6,5]	−0.000 004 48
14	−50.140 665 97	[6,6]	−0.000 007 76
15	−75.253 383 30	[7,6]	−0.000 003 28
16	−350.416 767 71	[7,7]	−0.000 002 33
17	−422.029 870 661	[8,7]	−0.000 002 85
18	−2869.728 624 743	[8,8]	−0.000 002 70
19	−2719.134 836 716	[9,8]	−0.000 002 78

rem implies a vanishing coupling between the $|1a_1^2 2a_1^2 1b_2^2\rangle$ and $|1a_1^2 2a_1^2 1b_2 2b_2\rangle$ interspace pair. Hence, the $|1a_1^2 2a_1^2 1b_2 2b_2\rangle$ state can then no longer act as an intruder state, and R_c may be enlarged. However, single excitations from the $|1a_1^2 2a_1^2 3a_1^2\rangle$ state may become important, possibly introducing an additional intruder state.

The divergent behavior of the single reference MBPT can also be explained from the complex z-dependent eigenvalue spectra obtained with barycentric–EN and MP partitioning (not shown here). For MP partitioning, the avoided crossing between the first and second states of $^1A_1$ symmetry occurs for positive Re z ($z_d \approx 0.95 \pm 0.14$), whereas for barycentric-EN partitioning it appears at negative Re z ($z_d \approx -0.51 \pm 0.01$). Both yield a radius of convergence $R_c = |z_d| < 1$ (0.96 for MP and 0.51 for EN) and imply a divergent SR perturbation series.

B. Asymptotic convergence with forced valence orbital degeneracy (FD) partitioning when using large reference space

Tables I through III demonstrate that FD partitioning for the double reference space state $(1\,^1A_1$ and $2\,^1A_1$ states) is convergent (through 30th order) over the entire potential surface, while the larger reference space computations (Sec. VII) yield usefully asymptotic series when truncated at low orders. The convergence of the perturbative series (not shown here) deteriorates rapidly with increasing size of the reference space. For example, at geometry B, the perturbative expansion for the $1\,^1A_1$ and $2\,^1A_1$ states begins to exhibit divergent behavior from the 23rd, 9th, 7th, and 5th order onwards for the three, four, five and six orbital reference spaces (described in the footnotes of Tables VII–IX), respectively. Although the deviation from the exact (FCI) value for the four, five and six-valence orbital reference

spaces is extremely large beyond the orders mentioned above, a well behaved series is obtained from these FD series through a Padé resummation procedure. Table IV clearly illustrates, how the Padé resummation procedure transforms the ''divergent'' FD series into (probably an) ''asymptotic'' series. Note that we truncate (i.e., stop computing) the perturbation expansion whenever the error in the $1\,^1A_1$ state energy (i.e., the deviation from the FCI value) exceeds 10^4 a.u. For instance, at geometry B, the deviation in the $1\,^1A_1$ state energy exceeds 10^4 a.u. at the 23rd, 20th, and 18th orders for the four, five, and six orbital reference spaces. Hence, we compute the Padé approximants only through order [11,10], [9,8], and [8,7] for the four, five and six orbital reference spaces, respectively. (The computation of [N,N-1] and [N,N]th order Padé approximants uses the perturbation expansion only through 2N+1 and 2N+2 th orders, respectively.) Tables V through VII display the low order Padé approximants for these FD series. Although, these tables quote the Padé appproximants through order [4,4], the higher order terms are well behaved up until the perturbation series becomes too unwieldy.

Except for small reference spaces, the FD partitioning yields some pairs of interspace states that have their zeroth order energies incorrectly ordered, producing divergent perturbation expansions. We illustrate this behavior only for the three valence orbital reference space of BeH₂, but similar patterns must occur with the larger (complete active) reference spaces. Furthermore, as discussed elsewhere,[52] the larger reference spaces may also have zeroth order energies between interspace states that are too close. Nevertheless, enlarging the reference space is shown to produce improved low order energies.

Figure 4 depicts the variation of $[E_m(z) - \bar{E}(z)]$ with Re z (Im z=0) for the first four eigenvalues of $^1A_1$ symmetry using the FD partitioning method and the three orbital reference space, where $E_m(z)$ is the z-dependent eigenvalue of

TABLE V. Energy errors $|E_{FCI}-E(N)|$ for the first $(1\,^1A_1)$ and second $(2\,^1A_1)$ BeH₂ $^1A_1$ states at geometry A using [N,M] Padé approximants and various reference spaces.

| Padé order [N,M] | FD partitioning method | | | OPT |
	Two orbital valence space	Four orbital valence space	Six orbital valence space	Two orbital valence space
$1\,^1A_1$				
[1,0]	0.030 420	0.023 146	0.005 875	0.017 557
[1,1]	0.018 243	0.003 053	0.001 355	0.00 1434
[2,1]	0.00 8123	0.007 413	0.000 605	0.006 204
[2,2]	0.014 718	0.003 179	0.000 169	0.004 289
[3,2]	0.002 101	0.002 010	0.000 093	0.008 330
[3,3]	0.000 290	0.005 537	0.000 094	0.001 056
[4,3]	0.000 318	0.000 261	0.000 093	0.000 279
[4,4]	0.000 293	0.000 798	0.000 009	0.000 196
$2\,^1A_1$				
[1,0]	0.032 760	0.008 192	0.003 181	0.001 098
[1,1]	0.007 094	0.007 384	0.002 852	0.002 482
[2,1]	0.004 193	0.008 329	0.000 288	0.001 411
[2,2]	0.001 410	0.001 132	0.000 602	0.000 024
[3,2]	0.001 319	0.000 210	0.000 367	0.000 324
[3,3]	0.001 417	0.000 017	0.001 049	0.000 152
[4,3]	0.000 049	0.00 0128	0.000 553	0.000 187
[4,4]	0.000 068	0.001 576	0.000 340	0.000 088

TABLE VII. Energy errors $|E_{FCI}-E(N)|$ for the first $(1\,^1A_1)$ and second $(2\,^1A_1)$ BeH₂ $^1A_1$ states at geometry C using [N,M] Padé approximants and various reference spaces.

| Padé order [N,M] | FD partitioning method | | | OPT |
	Two orbital valence space	Four orbital valence space	Six orbital valence space	Two orbital valence space
$1\,^1A_1$				
[1,0]	0.024 171	0.002 162	0.002 977	0.015 414
[1,1]	0.002 665	0.007 609	0.001 993	0.003 353
[2,1]	0.001 241	0.004 534	0.000 135	0.003 571
[2,2]	0.002 366	0.001 087	0.000 498	0.000 055
[3,2]	0.001 679	0.001 391	0.000 256	
[3,3]	0.000 476	0.000 034	0.000 221	0.000 980
[4,3]	0.000 852	0.000 072	0.000 152	
[4,4]	0.000 067	0.000 037	0.000 000	0.000 024
$2\,^1A_1$				
[1,0]	0.037 538	0.035 019	0.002 230	0.013 364
[1,1]	0.017 007	0.002 408	0.001 323	0.001 259
[2,1]	0.007 000	0.007 640	0.000 081	0.003 141
[2,2]	0.056 461	0.004 402	0.000 320	0.002 190
[3,2]	0.003 998	0.004 144	0.000 160	
[3,3]	0.000 282	0.004 427	0.000 004	0.000 264
[4,3]	0.000 370	0.000 418	0.000 382	0.000 086
[4,4]	0.000 302	0.000 584	0.000 037	0.000 051

the mth $^1A_1$ state and $\bar{E}(z)$ is the average of the first eight low-lying state energies. The presence of an avoided crossing is clearly visible in Fig. 4 between the $3\,^1A_1$ (P–corresponding) and the $4\,^1A_1$ (Q–corresponding) states near Re $z=0.80$. Detailed analysis confirms that the $3\,^1A_1$ and $4\,^1A_1$ are indeed degenerate (see Fig. 5) for $z_d \approx 0.875 \pm 0.04i$, yielding $R_c = 0.876$. In the vicinity of z_d, these two degenerate states are dominated by the zeroth

order $|1a_1^2 2a_1^2 1b_1^2\rangle$ (P space) and $|1a_1^2 2a_1 3a_1 1b_2^2\rangle$ (Q space) states for FD partitioning.

In order to explain and model the FD divergence we examine the two state model composed of the $|1a_1^2 2a_1^2 1b_1^2\rangle$ and $|1a_1^2 2a_1 3a_1 1b_2^2\rangle$ interspace pair, since these states dominate in the description of the $3\,^1A_1$ (P–corresponding) and the $4\,^1A_1$ (Q–corresponding) states near z_d for the full computation involving all states. The

TABLE VI. Energy errors $|E_{FCI}-E(N)|$ for the first $(1\,^1A_1)$ and second $(2\,^1A_1)$ BeH₂ $^1A_1$ states at geometry B using [N,M] Padé approximants and various reference spaces.

| Padé order [N,M] | FD partitioning method | | | OPT |
	Two orbital valence space	Four orbital valence space	Six orbital valence space	Two orbital valence space
$1\,^1A_1$				
[1,0]	0.030 685	0.012 568	0.003 529	0.021 948
[1,1]	0.025 155	0.007 751	0.001 852	0.001 198
[2,1]	0.006 402	0.017 404	0.000 118	0.004 024
[2,2]	0.004 429	0.002 479	0.000 375	0.002 610
[3,2]	0.001 921	0.002 427	0.000 081	0.000 949
[3,3]	0.000 227	0.002 481	0.000 997	0.001 586
[4,3]	0.001 928	0.000 436	0.000 990	0.000 282
[4,4]	0.000 645	0.000 082	0.000 643	0.000 731
$2\,^1A_1$				
[1,0]	0.031 958	0.023 142	0.003 227	0.007 172
[1,1]	0.003 426	0.007 062	0.002 252	0.004 221
[2,1]	0.001 216	0.011 864	0.000 117	0.005 076
[2,2]	0.001 863	0.000 389	0.000 543	0.004 591
[3,2]	0.002 756	0.001 506	0.000 292	0.005 822
[3,3]	0.002 024	0.001 232	0.000 076	0.000 645
[4,3]	0.001 616	0.001 160		0.000 358
[4,4]		0.001 268	0.000 083	0.000 176
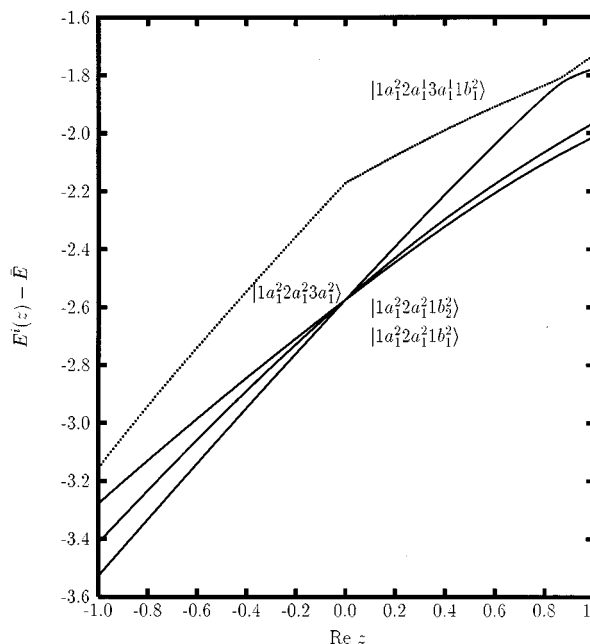
FIG. 4. First four $^1A_1$ state z–dependent eigenvalues of BeH₂ for geometry B from FD partitioning method (with three valence orbital reference space).
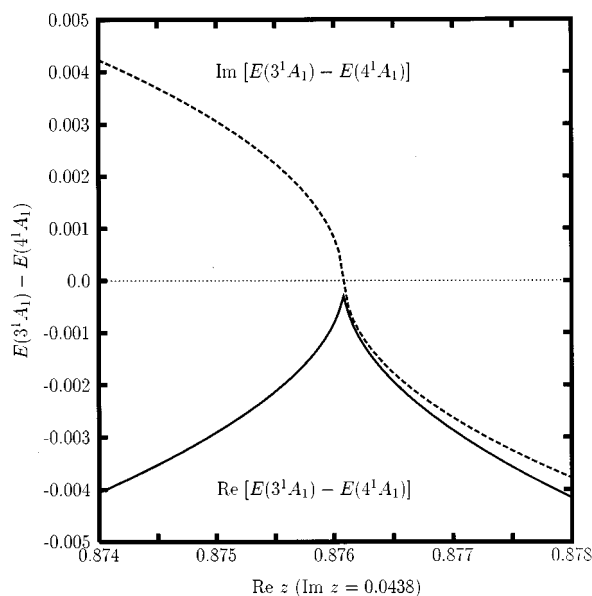
FIG. 5. z-dependent excitation energy $E(3\,^1A_1) - E(4\,^1A_1)$ of BeH$_2$ for geometry B from FD partitioning scheme (with three valence orbital reference space).

zeroth order energies of these two interspace states are incorrectly ordered with respect to their expectation values of H in a CSF basis. (See Sec. IV for a discussion on incorrect energy ordering.) Since there is no coupling between these states, the radius of convergence is infinite for a perturbative computation exclusively involving these two states. However, if a third state is added and if this state is coupled to both states even by an infinitesimal matrix element, then R_c is given by Eq. (4.7). This model yields R_c (z_d) as 0.95 $(0.95 \pm 0.0i)$, which is quite close to that for the full 197 CSFs computation. Hence, the divergence for the full problem is caused by incorrect energy ordering with the $|1a_1^2 2a_1 3a_1 1b_2^2\rangle$ ($|1a_1^2 2a_1^2 1b_1^2\rangle$) state acting as the intruder (escaping) state. Thus, we again find (with few exceptions) that a simple two or few state interspace model provides reasonable information regarding the high order convergence behavior of the MR-MBPT procedure and also the coupled states that are responsible for the poor convergence. Hence, the interspace two state models should provide a useful diagnostic for choosing reference spaces in applications of MR-MBPT, just as second order perturbation theory is used for choosing reference configurations for MRCI methods.

VII. $^1A_1$ STATE VERTICAL EXCITATION ENERGIES FROM THE LARGER REFERENCE SPACES

Table VIII displays the computed third order $1\,^1A_1 \rightarrow 2\,^1A_1$ vertical excitation energy from the forced degeneracy MR-MBPT for various choices of reference spaces, ranging from two to six orbital valence spaces, as well as from the OPT scheme for the two orbital valence space. We also present the multiconfigurational coupled cluster (MCCC) results of Bannerjee and Simons,[57] the quasidegenerate MR-MBPT(QD-MBPT) computation of Lee and

TABLE VIII. Vertical ($1\,^1A_1 \rightarrow 2\,^1A_1$) excitation energies (in eV) for different MR computational methods. [Values in parentheses are the absolute deviations (in eV) from the FCI, and the third order values are quoted for the FD and OPT methods.]

| Methods | Geometry | | | |
	A	B	C	Δ^a
FCI	2.6615	1.3217	2.4337	
MCCC[b]	2.6518	1.3293	2.4558	
	(0.010)	(0.008)	(0.022)	0.013
QD-MBPT[c]	3.2110	1.6109	2.2259	
	(0.456)	(0.291)	(0.202)	0.349
FD[d]	3.1610	1.6381	2.2798	
	(0.500)	(0.316)	(0.154)	0.323
FD[e]	3.0576	1.5798	2.2646	
	(0.396)	(0.258)	(0.169)	0.274
FD[f]	2.6545	1.3851	2.5577	
	(0.007)	(0.063)	(0.124)	0.065
FD[g]	2.7565	1.3566	2.4224	
	(0.095)	(0.035)	(0.011)	0.047
FD[h]	2.6864	1.3330	2.3986	
	(0.025)	(0.011)	(0.035)	0.024
FD[i]	2.6589	1.3154	2.4226	
	(0.003)	(0.006)	(0.011)	0.007
OPT	2.6378	1.3362	2.3569	
	(0.024)	(0.015)	(0.077)	0.039

[a]Average absolute deviation (in eV) from FCI.
[b]Reference 58.
[c]Reference 55.
[d]Two orbital valence space: $(core)^2 2a_1^2 [3a_1 1b_2]^2$.
[e]Three orbital valence space: $(core)^2 2a_1^2 [3a_1 1b_1 1b_2]^2$.
[f]Four orbital valence space: $(core)^2 [2a_1 3a_1 1b_1 1b_2]^4$.
[g]Five orbital valence space: $(core)^2 2a_1 [3a_1 4a_1 1b_1 1b_2 2b_2]^2$.
[h]Six orbital valence space: $(core)^2 [2a_1 3a_1 4a_1 1b_1 1b_2 2b_2]^4$.
[i]Seven orbital valence space: $(core)^2 [2a_1 3a_1 4a_1 5a_1 1b_1 1b_2 2b_2]^4$.

Bartlett,[54] and the FCI value to evaluate the relative performance of the different approaches. (Since the absolute state energy is not a bound in perturbative methods, Table VIII compares excitation energies.) Tables IX and X present the third order $1\,^1A_1 \rightarrow 3\,^1A_1$ and $1\,^1A_1 \rightarrow 4\,^1A_1$ vertical excita-

TABLE IX. Third order vertical ($1\,^1A_1 \rightarrow 3\,^1A_1$) excitation energies (in eV) for FD schemes. [Values in parentheses are the absolute deviations (in eV) from the FCI.]

| Methods | Geometry | | | |
	A	B	C	Δ^a
FCI	6.4432	6.3895	7.2327	
FD[b]	6.5963	6.6579	7.9361	
	(0.153)	(0.268)	(0.703)	0.375
FD[c]	6.4646	6.4835	7.2911	
	(0.021)	(0.094)	(0.058)	0.058
FD[d]	6.4111	6.3957	7.2468	
	(0.032)	(0.006)	(0.013)	0.017
FD[e]	6.4214	6.3697	7.2276	
	(0.022)	(0.020)	(0.005)	0.016

[a]Average absolute deviation (in eV) from FCI estimate.
[b]Four orbital valence space: $(core)^2 [2a_1 3a_1 1b_1 1b_2]^4$.
[c]Five orbital valence space: $(core)^2 2a_1 [3a_1 4a_1 1b_1 1b_2 2b_2]^2$.
[d]Six orbital valence space: $(core)^2 [2a_1 3a_1 4a_1 1b_1 1b_2 2b_2]^4$.
[e]Seven orbital valence space: $(core)^2 [2a_1 3a_1 4a_1 5a_1 1b_1 1b_2 2b_2]^4$.

TABLE X. Third order vertical ($1\ ^1A_1 \rightarrow 4\ ^1A_1$) excitation energies (in eV) for FD schemes. [Values in parentheses are the absolute deviations (in eV) from the FCI.]

Methods	Geometry			
	A	B	C	Δ^a
FCI	8.6799	7.6016	7.7815	
FD[b]	9.2559	8.2619	8.5733	
	(0.576)	(0.660)	(0.792)	0.676
FD[c]	8.9589	7.6759	7.9886	
	(0.279)	(0.074)	(0.207)	0.187
FD[d]	8.7698	7.6635	7.7835	
	(0.090)	(0.062)	(0.002)	0.051
FD[e]	8.6737	7.6001	7.7704	
	(0.006)	(0.001)	(0.011)	0.006

[a]Average absolute deviation (in eV) from FCI estimate.
[b]Four orbital valence space: $(core)^2[2a_1 3a_1 1b_1 1b_2]^4$.
[c]Five orbital valence space: $(core)^2 2a_1[3a_1 4a_1 1b_1 1b_2 2b_2]^2$.
[d]Six orbital valence space: $(core)^2[2a_1 3a_1 4a_1 1b_1 1b_2 2b_2]^4$.
[e]Seven orbital valence space: $(core)^2[2a_1 3a_1 4a_1 5a_1 1b_1 1b_2 2b_2]^4$.

tion energies, respectively, as obtained using four, five and six orbital valence spaces. Almost all the FD partitioning computations display the general trend that the accuracy of the third order excitation energies, i.e., the deviation from the FCI excitation energies, improves with an increase in the size of the reference space. For example, the average absolute deviation (for geometries A, B, and C) in the third order excitation energy for the $1\ ^1A_1 \rightarrow 2\ ^1A_1$ transition is only 0.024 eV with the six orbital reference space as compared to 0.047 with the five orbital reference space. The improvement is also substantial for higher excited states, even though the larger reference space computations are only asymptotic and begin diverging earlier than in the calculations with smaller reference spaces. These divergent series, however, are transformed to a useful asymptotic form by Padé resummation techniques. Similar patterns are also found for several other geometries along the reaction path of BeH₂. The trends described above often appear since an increase in the size of the the reference space improves the first order description [given by the first two terms on the right hand side of Eq. (2.13)] and reduces the remaining ''correlation contribution'' [from the sums in Eq. (2.13)] to be obtained perturbativly. Thus a seven valence orbital reference space produces almost FCI accuracy at third order (but only two excited orbitals remain) and offers a decent asymptotic perturbation series. Although the perturbative series diverge more rapidly (see Sec. VI B) with the larger than the smaller reference spaces (especially for the higher excited states), the high order divergence does not degrade the accuracy of the lower lying states in low orders.

VIII. $^1A_1$ STATE VERTICAL EXCITATION ENERGIES FOR OPT PARTITIONING

The OPT method converges much faster than with the FD partitioning approach for the two orbital valence space or the QD-MBPT calculations of Bartlett *et al.*[54] The accuracy of the two orbital valence space OPT treatment lies some-

what in between that of the five and six valence orbital reference space calculations within the FD scheme. Because of this high accuracy, we have not considered OPT treatments with larger reference spaces.

IX. DISCUSSION

The third order, two valence orbital space FD calculation closely resembles that from the OPT partitioning method and from the QD-MBPT approach of Lee and Bartlett. These three schemes differ only in the choice of zeroth order energies and the orbitals. All three employ the same number of valence orbitals in the reference space and, hence, the same configuration state functions in the reference space. All three methods generate a convergent perturbative series through 30th order. However, the low order (e.g., third order) results differ significantly. For example, the FD partitioning method offers an improved result, i.e., a smaller deviation of the excitation energy from the FCI than from the QD-MBPT method, but an even more significant improvement in the excitation energy is obtained by OPT method. The excitation energy computed with the OPT scheme is comparable to the highly correlated MCCC and FD partitioning methods with a six valence orbital reference space whose dimension is almost half of the FCI space. Also, the OPT scheme provides a more rapidly convergent perturbative series than the double reference QD-MBPT and FD-MBPT methods. This demonstrates that the accuracy and convergence of the MR-MBPT method depends on the choice of the zeroth order energies. (Note that the H_0 formed with unaveraged IVO orbital energies also yields a convergent double reference perturbative series and is to some extent better than the FD-series, a finding in accord with small valence space H^v computations demonstrating improved results in truly quasidegenerate situations when valence orbital energy averaging may be avoided.)

Table VIII indicates that as the size of the reference space grows, the accuracy of the FD method increases. The trend in Table VIII is not surprising, since the larger reference space computation offers a better first order description and requires a smaller correlation correction. On the other hand, as the size of the reference space increases, the quasidegeneracy of the valence orbital energies diminishes. Therefore, a large diagonal perturbation matrix element appears, with additional energy denominators that may be too small,[52] due to the forced valence orbital degeneracy restriction. (See Ref. 22 for details.) Hence, it is not surprising the the larger reference spaces exhibit divergent behavior in earlier orders for the FD partitioning perturbative series (although Padé resummations improve matters considerably). Enlarging the valence space involves a trade-off, and the success of FD method depends on the relative importance of the opposing factors. When the diagonal perturbation is too large or when small energy denominators appear, the convergence and accuracy of FD partitioning may degrade. In fact, the success of the FD scheme lies mostly on the appropriate selection of the reference space, a process which requires some trial and error searching and *a priori* knowledge of the

most important configurations. Recent computations for two-dimensional methyl mercaptan[51] and three-dimensional hydrogen sulfide[61] potential energy surfaces establish that once the appropriate reference is obtained, the FD method not only provides accurate excitation energies (for both Rydberg and valence states), ionization energies, and dissociation energies but also generates accurate potential energy surfaces even with a limited number of valence space orbitals.

X. CONCLUSIONS

The present high order multireference perturbative computations further emphasize the utility of two state models for providing convergence criteria and for assessing the quality of possible choices for partitioning methods, orbitals, etc. An analysis of all interspace two state models composed of higher lying P-space states and lower lying Q-space states, provides an indication of probable impediments to the perturbative convergence and of possible remedies for these problems. This type of analysis bear some relation to the perturbative criterion for selecting reference space configurations for multireference CI methods in its simplicity and general utility. However, it is important to mention that situations may arise where the two state model is inadequate to describe the perturbative divergence problems and where higher dimensional models are required. These situations may occur when more than one Q-space state is important because they are strongly coupled among themselves and to the higher lying P space. The optimized partitioning method (OPT) discussed here may not resolve all the problems with the MR-MBPT method but may provide a useful alternative tool to tackle the perturbative convergence problem by adjusting the state energies for the high lying P-space and low lying Q-space states. Further attempts should be made to optimize the orbital energies instead of the state energies. Optimization of the orbital energies affects more states and, in addition, generates a method that preserves size extensivity. The forced degeneracy (FD) method is again shown to alleviate the most serious intruder state problems plaguing general multireference methods.

Since our computations have covered a wide range of geometries (not presented) and reference spaces, we have made a preliminary investigation of the possibility for piecing together the potential energy surfaces using different reference spaces in different regions. The approach has been quite successful when applied with the four and five orbital reference spaces, and we surmise that smooth surfaces can only be obtained when there exists a common overlapping region of geometries for which both reference spaces provide comparable accuracy. However, more extensive tests are required to establish more general criteria for the use of multiple reference spaces to produce smooth global potential energy surfaces.

ACKNOWLEDGMENT

[1] K. A. Bruckner, Phys. Rev. **97**, 1353 (1955).
[2] J. Goldstone, Proc. R. Soc. London Ser. A **239**, 267 (1957).
[3] N. M. Hugenholtz, Physica **27**, 281 (1957).
[4] J. Hubbard, Proc. R. Soc. London Ser. A **240**, 539 (1957).
[5] F. Cöester, Nucl. Phys. **7**, 421 (1958).
[6] F. Cöester and H. Kümmel, Nucl. Phys. **17**, 477 (1960).
[7] H. Kümmel, K. H. Luhrmann, and J. G. Zabolotzky, Phys. Rep. **36**, 1 (1978).
[8] N. C. Handy, P. J. Knowles, and K. Somasudram, Theor. Chim. Acta **68**, 87 (1985).
[9] R. J. Bartlett and G. D. Purvis, Int. J. Quantum Chem. **14**, 561 (1978).
[10] R. J. Bartlett and G. D. Purvis, Phys. Scr. **21**, 255 (1980).
[11] B. Brandow, Rev. Mod. Phys. **39**, 771 (1967).
[12] P. Sandars, Adv. Chem. Phys. **14**, 365 (1969).
[13] V. Kvasnička, Czech J. Phys. B **24**, 605 (1974).
[14] I. Lindgren, J. Phys. B **7**, 2441 (1974).
[15] I. Lindgren and J. Morrison, *Atomic Many-Body Theory*, 2nd ed, Springer Series on Atoms and Plasmas (Springer, New York, 1986).
[16] G. Oberlechner, F. Owon-N-Cuema, and J. Richert, Nuovo Cimento B **68**, 23 (1970).
[17] T. T. S. Kuo, S. Y. Lee, and K. F. Ratcliff, Nucl. Phys. A **176**, 65 (1971).
[18] M. Johnson and B. Barangar, Ann. Phys. **62**, 172 (1971).
[19] D. M. A. Bannerjee and J. Simons, J. Chem. Phys. **76**, 1979 (1982).
[20] T. H. Schucan and H. A. Weidenmüller, Ann. Phys. (N.Y.) **73**, 108 (1972).
[21] T. H. Schucan and H. A. Weidenmüller, Ann. Phys. (N.Y.) **76**, 483 (1973).
[22] J. P. Finley, R. K. Chaudhuri, and K. F. Freed, Phys. Rev. A **54**, 343 (1996).
[23] G. Hose and U. Kaldor, J. Phys. B **12**, 3827 (1979).
[24] M. Sheppard, J. Chem. Phys. **80**, 1225 (1984).
[25] R. Chaudhuri, D. Sinha, and D. Mukherjee, Chem. Phys. Lett. **163**, 165 (1989).
[26] D. Mukherjee, Proc. Ind. Acad. Sci. **96**, 145 (1986).
[27] D. Mukherjee, Chem. Phys. Lett. **125**, 207 (1986).
[28] J. P. Malrieu, P. Durand, and J. P. Daudey, J. Phys. A **18**, 809 (1985).
[29] S. Wilson, K. Jankowski, and J. Paldus, Int. J. Quantum. Chem. **23**, 1781 (1983).
[30] S. Wilson, K. Jankowski, and J. Paldus, Int. J. Quantum. Chem. **28**, 525 (1986).
[31] S. Zarrabian and J. Paldus, Int. J. Quantum. Chem. **38**, 761 (1990).
[32] D. M. Silver and R. J. Bartlett, Phys. Rev. A **13**, 1 (1976).
[33] D. M. Silver, S. Wilson, and R. J. Bartlett, Phys. Rev. A **16**, 477 (1977).
[34] C. W. Murray and E. R. Davidson, Int. J. Quantum Chem. **43**, 755 (1992).
[35] K. Andersson, P. Å. Malmqvist, and B. O. Roos, J. Chem. Phys. **96**, 1218 (1992).
[36] M. P. Fülscher, K. Andersson, and B. O. Roos, J. Chem. Phys. **96**, 9204 (1992), and references therein.
[37] K. Wolinski and P. Pulay, J. Chem. Phys. **90**, 3647 (1989).
[38] M. R. Hoffmann, J.Phys. Chem. **100**, 6125 (1996).
[39] D. Mukhopadhyay, B. Datta, and D. Mukherjee, Chem. Phys. Lett. **197**, 236 (1992).
[40] J. P. Malrieu, J. L. Heully, and A. Zaitsevski, Theor. Chim. Acta. **90**, 167 (1995).
[41] A. V. Zaitsevskii and J.-L. Heully, J. Phys. B **25**, 603 (1992).
[42] G. Jolicard and G. D. Billing, J. Phys. B **23**, 3457 (1990).
[43] J. P. Malrieu and A. Zaitsevski, Chem. Phys. Lett. **233**, 597 (1995).
[44] H. Sun, M. G. Sheppard, and K. F. Freed, J. Chem. Phys. **74**, 6842 (1981).
[45] Y. S. Lee and K. F. Freed, J. Chem. Phys. **77**, 1984 (1982).
[46] X.-C. Wang and K. F. Freed, J. Chem. Phys. **86**, 2899 (1987).
[47] X. C. Wang and K. F. Freed, J. Chem. Phys. **91**, 3002 (1989).
[48] K. F. Freed, *Lecture Notes in Chemistry* (Springer, Berlin, 1989), Vol. 52, p. 1.
[49] R. L. Graham and K. F. Freed, J. Chem. Phys. **96**, 1304 (1992).
[50] C. H. Martin, R. L. Graham, and K. F. Freed, J. Chem. Phys. **99**, 7833 (1993).
[51] J. E. Stevens, K. F. Freed, M. F. Ardent, and R. L. Graham, J. Chem. Phys. **101**, 4832 (1994).
[52] J. P. Finley and K. F. Freed, J. Chem. Phys. **102**, 1306 (1995).
[53] J. P. Finley, R. K. Chaudhuri, and K. F. Freed, J. Chem. Phys. **103**, 4990 (1995).
[54] Y. S. Lee and R. J. Bartlett, Int. J. Quantum Chem. S **17**, 347 (1983).

[55] G. D. Purvis, R. Sheppard, F. B. Brown, and R. J. Bartlett, Int. J. Quantum Chem. **23**, 835 (1983).

[56] S. Zarrabian, W. D. Laidig, and R. J. Bartlett, Phys. Rev. A **41**, 4711 (1990).

[57] A. Banerjee and J. Simons, Chem. Phys. **87**, 215 (1984).

[58] M. R. Hoffmann, X.-C. Wang, and K. F. Freed, Chem. Phys. Lett. **136**, 392 (1987).

[59] S. Y. Lee and K. F. Freed, J. Chem. Phys. **104**, 3260 (1996).

[60] R. K. Chaudhuri and K. F. Freed (unpublished).

[61] J. E. Stevens, R. K. Chaudhuri, and K. F. Freed, J. Chem. Phys. **105**, 8754 (1996).

[62] B. Huron, P. Rancurel, and J. P. Malrieu, J. Chem. Phys. **58**, 5745 (1973).

[63] S. Wilson, K. Jankowski, and J. Paldus, Int. J. Quantum Chem. **28**, 525 (1985).

[64] J. M. Leinaas and T. T. S. Kuo, Phys. Lett. B **62**, 275 (1976).

[65] P. J. Ellis and E. Osnes, Rev. Mod. Phys. **49**, 777 (1977).